DRAGON SOLUTIONS FOR BENCHMARK BWR LATTICE CELL PROBLEMS

R. Roy and G. Marleau
Institut de Génie Nucléaire
École Polytechnique de Montréal
P.O.Box 6079, Station CV, Montreal, Canada
roy@meca.polymtl.ca ; marleau@meca.polymtl.ca

ABSTRACT

The classical NEACRP benchmark BWR lattice cell problems are analysed using the DRAGON cell code. These benchmark problems are assemblies of pin cells with given six-group cross sections. Our results are compared with available published solutions. The first goal of our comparison is to assess the two most accurate methods of solution in DRAGON for 2-D reflected lattice. The second goal is to evaluate the effect of boundary conditions, namely isotropic and specular reflection, on the precision of the solutions. Numerical results show a very good agreement between DRAGON and other modern codes. Changing the type of boundary conditions leads to notable fission-map differences only in cases where an absorber is located near the external boundary and generally results in minor effects on the accuracy.

1. INTRODUCTION

In this paper, the NEACRP benchmark BWR lattice cell problems[1] will be analysed using modules available in the DRAGON[2] cell code. Among all the solution options available in DRAGON for 2-D reflected lattice problems, only the collision probability technique with isotropic boundary conditions (CP/I) and the method of characteristics with specular reflection (MOCC/S) were selected. Each of these methods works using the following modules.

For the CP/I calculations, we used:

- the EXCELT module to generate finite tracks up to the external assembly boundary;
- the ASM module to compute the heterogeneous (collision, escape and transmission) probabilities and to built the complete CP matrix using isotropic reflections;
- the FLU module to solve the resulting multigroup CP equations.

Similarly, the MOCC/S calculations were performed using:

- the EXCELT module to generate the infinite integration lines associated with the infinite geometry generated from the reference lattice using mirror-like reflections;

- the MOCC module to solve the transport equation using the method of cyclic characteristics.[3]

Note that there also exists in DRAGON a version of the collision probability technique that can deal with specular boundary conditions (CP/S).[4] However, since both the MOCC/S and CP/S techniques give identical results, we will restrict our analysis to the former method that does not require the collision probability matrices calculations and the linear system FLU solver.

The main objective of this work is to show the agreement between the DRAGON results and published solutions when similar meshing and tracking approximations can be made. Another goal is to analyse the result sensitivity on boundary conditions either taken as isotropic or specular; that is to measure the importance of the neutron direction when leaving the boundary.

2. NUMERICAL RESULTS

2.1 BURNABLE POISON SUPERCELL PROBLEM

Our first results will be presented for Problem 1, which represents a 3x3 array of pin cells with a central poison pin.[1] This poison pin supercell is thus composed of the central pin containing fuel with gadolinia poison surrounded by 8 normal fuel pins in a square lattice of pitch 1.87452 cm. In order to compare our solutions to those given in reference 5, a regular 3x3 Cartesian submeshing was superimposed over each pin cell. The EXCELT tracking was performed using a reference density of 400 lines/cm with 40 azimuthal angles for the isotropic tracking and a M19 quadrature set for the specular tracking (see reference 3).

For the cases where the specular method is used (MOCC/S), the additional integration in the polar direction was performed using Gauss-Legendre quadrature.[3] Note that the dependence in k-infinite values on the number of azimuthal angles or the type of cyclic quadrature set is relatively weak. In fact, the use of 20 rather than 40 azimuthal angles in the isotropic CP/I calculation yields a reduction in k-infinite of 4 pcm while taking a T19 instead of a M19 cyclic quadrature set results in a change of around 8 pcm in reactivity.

In Table I, we give our best estimates for k-infinite and reaction rates for this problem (absorption by material and fission cell map) using the tracking parameters previously described. In Figure 1, we plot Gd absorption rate (material 4, 5 and 6) versus k-infinite; one can see that both DRAGON results lie near the same linear curve as other authors' values but not exactly at the same level.

Table I. Results for BWR supercell Problem 1.

	CLUP77 (reference 1)	AEEW (reference 1)	MAGGENTA (reference 5)	ANEMONA (reference 5)	MOCC/S (this work)	CP/I (this work)
k-infinite	0.8768	0.8825	0.8761	0.8799	0.8775	0.8763
Absorption rates						
Material 1	0.7241	0.7269	0.7237	0.7258	0.7243	0.7238
Material 2	0.0105	0.0106	0.0105	0.0105	0.0105	0.0105
Material 3	0.0223	0.0226	0.0222	0.0222	0.0223	0.0222
Material 4	0.0600	0.0579	0.0595	0.0592	0.0593	0.0595
Material 5	0.0405	0.0393	0.0409	0.0406	0.0408	0.0409
Material 6	0.1390	0.1392	0.1397	0.1382	0.1392	0.1396
Material 7	0.0012	0.0012	0.0012	0.0012	0.0012	0.0012
Material 8	0.0024	0.0023	0.0023	0.0023	0.0024	0.0024
Fission rate map						
Central pin	0.515	0.499	0.508	0.505	0.507	0.508
Bottom pins	1.043	1.038	1.041	1.039	1.041	1.041
Corner pins	1.078	1.087	1.082	1.084	1.082	1.082

As expected, the CP/I results (isotropic reflection) are very similar to those obtained using MAGGENTA, a fact that is not surprising since both evaluations use the same general solution technique and similar meshing. However, the MOCC/S results (or equivalently the specular CP/S method) are quite different from those generated by ANEMONA. This could be caused by the approximation taken at the boundary: incident rays are just specularly reflected in DRAGON while in ANEMONA an average value of the incident rays on each boundary edge is taken as the value of the reflected angular flux.[4] Although both DRAGON solvers use quite different methodologies, there is a good agreement between the last two columns of Table 1. The spread in solutions between the MOCC/S and CP/I solvers indicates that the effect of boundary conditions is about 120 pcm in this particular problem.

Table II. Comparison of multiplication factors and absorption rates in Problem 1 for various quadratures used in the MOCC/S solver.

	Azimuthal angles	
Polar angles	M19 cyclic quadrature	T19 cyclic quadrature
k-infinite		
2 optimal	0.87768	0.87781
10 Gauss-Legendre	0.87752	0.87764
Absorption rate in materials 4+5+6		
2 optimal	0.23925	0.23922
10 Gauss-Legendre	0.23935	0.23932

For the cases where the specular method is used, calculations were repeated using the same two optimal polar angles used in CHAR or ANEMONA.[5] In Table II, results obtained with various quadrature sets are given, and it is obvious that the use of two polar angles is sufficient to obtain a good accuracy (about 10 pcm for k-infinite).

2.2 'MINI-BWR' WITH DIFFERENTIAL ENRICHMENT AND CRUCIFORM ABSORBER

This 'mini-BWR' problem (labeled Problem 2) consists of a 2x2 array of pin cells containing a range of enrichments, surrounded by their associated coolant and a simulated cruciform control rod. Our best estimate results are based on the same mesh splitting (3x3 superimposed cartesian mesh over each cell) and tracking parameters are identical with those of the previous problem: 40 azimuthal angles in the CP method, the M19 cyclic quadrature with 10 Gauss polar angles, and a track density of 400 lines/cm.

In Table III, we compare k-infinite and absorption rates. The difference between the isotropic and specular boundary conditions is only of 14 pcm in reactivity (with similar changes for absorption rates in the rod).

Table III. Results for BWR Problem 2.

	CLUP77 (reference 1)	AEEW (reference 1)	MOCC/S (this work)	CP/I (this work)
k-infinite	0.8078	0.8200	0.8182	0.8184
Absorption rates				
Material 1	0.1496	0.1533	0.1516	0.1521
Material 2	0.0019	0.0020	0.0020	0.0020
Material 3	0.0095	0.0098	0.0096	0.0097
Material 4	0.3097	0.3144	0.3136	0.3143
Material 5	0.0036	0.0037	0.0037	0.0037
Material 6	0.0167	0.0170	0.0169	0.0170
Material 7	0.1321	0.1305	0.1317	0.1306
Material 8	0.0015	0.0015	0.0015	0.0015
Material 9	0.0056	0.0055	0.0055	0.0054
Material 10	0.3466	0.3387	0.3403	0.3402
Material 11	0.0231	0.0237	0.0235	0.0235
Fission rate map				
Pin near rod	0.896	0.871	0.881	0.872
Pin far rod	0.980	0.988	0.985	0.990
Other pins	1.062	1.070	1.067	1.069

The k-infinite discrepancy has no significant effect on the material absorption rates (except maybe for material 7); however, the fission rates show an evident trend: the isotropic reflection approximation has for effect to reduce the fission rate for pins close to the control rod.. In Figure 2, we can still remark that MOCC/S and CP/I solvers gives almost the same point along the absorption in cruciform rod versus k-infinite curve, almost on the straight line formed by the CLUP77 and AEEW points.

In Table IV, the dependence of the MOCC/S results on the specific quadrature sets is again analysed. One can note that the number of polar angles selected is now an important parameter; the difference in reactivity between our reference solution and the one obtained using the 2 optimal polar angle is now of about 50 pcm. The most probable explanation is that the

appreciation of the local changes in high absorption regions is not well represented by the average values used by fewer polar angles, so that the neutron optical path integration required by the MOCC/S technique is outside the range for which these two optimal polar angles were selected.

Table IV. Comparison of multiplication factors and absorption rates in Problem 2 for various quadratures used in the MOCC/S solver.

	Azimuthal angles	
Polar angles	M19 cyclic quadrature	T19 cyclic quadrature
k-infinite		
2 optimal	0.81872	0.87878
10 Gauss-Legendre	0.81821	0.81828
Absorption rate in materials 3+6+9		
2 optimal	0.03213	0.03213
10 Gauss-Legendre	0.03208	0.03208

2.3 BWR LATTICE CELL WITH POISONED FUEL PINS

The third benchmark (labeled Problem 3 in reference 1) represents a 7x7 array containing 6 different pin types with several fuel enrichments and some poisoned fuel pins. Our best estimates results are given in Table V. A superimposed 2x2 Cartesian grid was put on each pin cell; this corresponds to split in four quadrant every pin-cell zone, as this meshing strategy was previously applied to the context of MOX-PWR assembly calculations with good accuracy.[6] Tracking parameters are similar to the previous ones, except that the density was reduced to 100 lines/cm. Numerical results of Table V show that there is no significant effect of the boundary conditions in this problem. If we choose to use the T19 quadrature instead of the M19 (reference) one, there is a slight change of 11 pcm in reactivity. However, the number of azimuthal angles can be significant: for example, the M7 and T7 cyclic quadrature sets give k-infinite values of 1.06039 and 1.06133 respectively (with a difference of 94 pcm), showing that such results are still not converged.

Table V. Results for BWR lattice-cell Problem 3.

	CLUP77 (reference 1)	AEEW (reference 1)	MOCC/S (this work)	CP/I (this work)
k-infinite	1.0579	1.0662	1.0607	1.0608
Absorption rates				
Material 1	0.2355	0.2348	0.2336	0.2336
Material 2	0.0025	0.0025	0.0025	0.0025
Material 3	0.0078	0.0078	0.0077	0.0077
Material 4	0.1453	0.1476	0.1464	0.1464
Material 5	0.0016	0.0017	0.0016	0.0016
Material 6	0.0058	0.0059	0.0059	0.0059
Material 7	0.1106	0.1133	0.1121	0.1121
Material 8	0.0014	0.0013	0.0013	0.0013
Material 9	0.0051	0.0052	0.0052	0.0052
Material 10	0.0189	0.0199	0.0195	0.0195
Material 11	0.0002	0.0003	0.0002	0.0002
Material 12	0.0011	0.0011	0.0011	0.0011
Material 13	0.1012	0.0984	0.1007	0.1007
Material 14	0.0006	0.0006	0.0006	0.0006
Material 15	0.0016	0.0016	0.0016	0.0016
Material 16	0.2472	0.2458	0.2461	0.2461
Material 17	0.0029	0.0029	0.0029	0.0029
Material 18	0.0077	0.0076	0.0076	0.0076
Material 19	0.0109	0.0112	0.0110	0.0110
Material 20	0.0349	0.0367	0.0354	0.0354
Material 21	0.0328	0.0308	0.0327	0.0327
Material 22	0.0246	0.0230	0.0244	0.0244

Once more, the CP/I and MOCC/S agreement with high orders of angular quadrature can be seen in Table VI, where fission maps given for both solvers are almost identical. These numerical results also agree the ones produced by the codes CASMO-3 and KRAM2D.[5]

Table VI. Fission rate map for BWR lattice-cell Problem 3.

					CLUP77 (reference 1)	1.115
					AEEW (reference 1)	1.184
					CASMO-3 (reference 5)	1.160
					KRAM2D (reference 5)	1.148
					MOCC/S (this work)	1.156
					CP/I (this work)	1.156
					1.090	1.179
					1.118	1.228
					1.112	1.197
					1.109	1.211
					1.112	1.210
					1.112	1.209
				0.914	1.079	1.031
				0.924	1.098	1.072
				0.926	1.087	1.043
				0.906	1.091	1.061
				0.915	1.094	1.054
				0.915	1.094	1.054
			0.809	0.821	0.308	1.097
			0.782	0.807	0.299	1.138
			0.815	0.811	0.304	1.100
			0.798	0.807	0.304	1.128
			0.805	0.817	0.308	1.116
			0.805	0.817	0.308	1.116
		0.822	0.788	0.859	1.006	1.130
		0.809	0.768	0.860	1.005	1.160
		0.818	0.773	0.865	1.001	1.144
		0.802	0.771	0.847	1.004	1.160
		0.809	0.779	0.855	1.009	1.147
		0.809	0.778	0.855	1.009	1.147
	1.040	0.895	0.300	0.945	1.167	1.233
	1.007	0.870	0.287	0.928	1.155	1.246
	1.035	0.873	0.292	0.927	1.179	1.236
	1.020	0.875	0.293	0.928	1.162	1.248
	1.022	0.879	0.296	0.933	1.164	1.240
	1.022	0.879	0.296	0.933	1.164	1.240
1.178	1.246	1.127	1.072	1.169	1.365	1.200
1.146	1.207	1.099	1.056	1.160	1.360	1.209
1.150	1.235	1.119	1.057	1.179	1.386	1.184
1.155	1.225	1.112	1.063	1.171	1.371	1.200
1.156	1.221	1.105	1.059	1.163	1.368	1.200
1.156	1.221	1.105	1.059	1.163	1.368	1.200

2.4 BWR LATTICE CELL WITH A CRUCIFORM ROD

The last benchmark problem, labeled Problem 4, represents a 8x8 array containing 4 different pin types with uranium, plutonium and poisoned fuel pins, one empty pin position and a homogenized cruciform rod. Our best results are obtained using the same spatial mesh splitting (2x2 superimposed grid on pin cell and empty position) and angular quadrature sets as in Problem 3.

In Table VII, we give k-infinite and absorption rates in the different materials. When the T19 quadrature is used rather than M19 in the MOCC/S solver, a 9 pcm difference in reactivity is observed, which indicates that our solution is converged. Here, the effect of boundary conditions can be estimated to 123 pcm.

Table VII. Results for BWR lattice-cell Problem 4.

	CLUP77 (reference 1)	AEEW (reference 1)	MOCC/S (this work)	CP/I (this work)
k-infinite	0.8175	0.8237	0.8182	0.8170
Absorption rates				
Material 1	0.1614	0.1612	0.1610	0.1606
Material 2	0.0033	0.0033	0.0033	0.0033
Material 3	0.0052	0.0052	0.0051	0.0051
Material 4	0.2034	0.1994	0.2002	0.1999
Material 5	0.0025	0.0024	0.0025	0.0025
Material 6	0.0032	0.0031	0.0031	0.0031
Material 7	0.0113	0.0108	0.0113	0.0112
Material 8	0.0157	0.0148	0.0157	0.0156
Material 9	0.0442	0.0447	0.0443	0.0442
Material 10	0.0005	0.0005	0.0005	0.0005
Material 11	0.0007	0.0007	0.0007	0.0007
Material 12	0.2938	0.3014	0.2972	0.2969
Material 13	0.0055	0.0055	0.0056	0.0056
Material 14	0.0099	0.0103	0.0101	0.0101
Material 15	0.0005	0.0005	0.0005	0.0005
Material 16	0.0060	0.0060	0.0061	0.0061
Material 17	0.0191	0.0202	0.0198	0.0198
Material 18	0.0150	0.0151	0.0149	0.0150
Material 19	0.1588	0.1544	0.1577	0.1587
Material 20	0.0264	0.0269	0.0267	0.0269
Material 21	0.0116	0.0118	0.0116	0.0115
Material 22	0.0021	0.0021	0.0021	0.0021

The fission rate map given in Table VIII exhibits a behavior similar to the one observed in Problem 2 (where there also was a rod): the relative fission rate is increased near the cruciform rod in the case of specular reflection.

Table VIII. Fission rate map for BWR lattice-cell Problem 4.

						CLUP77 (reference 1)	0.671
						AEEW (reference 1)	0.662
						MOCC/S (this work)	0.660
						CP/I (this work)	0.648
						0.638	0.650
						0.630	0.640
						0.627	0.636
						0.618	0.625
					0.302	0.620	0.646
					0.299	0.612	0.634
					0.300	0.609	0.629
					0.297	0.602	0.620
				1.088	1.066	0.653	0.672
				1.040	1.027	0.643	0.660
				1.055	1.037	0.640	0.654
				1.052	1.030	0.634	0.647
			empty	1.202	1.183	0.717	0.736
			pin	1.161	1.147	0.705	0.725
			location	1.172	1.152	0.705	0.718
				1.172	1.148	0.700	0.712
		1.685	1.471	1.289	1.357	0.817	0.856
		1.645	1.447	1.232	1.333	0.812	0.851
		1.660	1.444	1.259	1.333	0.815	0.847
		1.672	1.451	1.261	1.331	0.812	0.842
	1.229	1.086	0.943	0.380	0.891	0.980	1.054
	1.237	1.079	0.946	0.380	0.897	0.990	1.076
	1.242	1.084	0.940	0.383	0.893	0.990	1.073
	1.256	1.093	0.945	0.384	0.893	0.989	1.072
1.593	1.421	1.292	1.180	1.098	1.133	1.198	1.306
1.652	1.458	1.317	1.211	1.141	1.170	1.244	1.380
1.665	1.464	1.319	1.205	1.130	1.159	1.236	1.373
1.692	1.481	1.329	1.209	1.130	1.157	1.235	1.379

As in the previous 7x7 assembly problem, the number of azimuthal angles can be significant: for example, the M7 and T7 cyclic quadrature sets give k-infinite values of 0.81762 and 0.81898 respectively (with a difference of 136 pcm).

CONCLUSIONS

In the perspective of comparing codes and validating their methodology, the analysis of simple benchmark problems is crucial. It was shown that, for all the NEACRP BWR benchmark problems, DRAGON results are consistent and in good agreement with other published solutions. In general, the effect of boundary conditions (locally isotropic or specular) is weak as long as the external boundary is sufficiently discretized. However, in cases where strong absorbers are present near the boundary, the eigenvalues and the fission maps can substantially change if we take into account the neutron direction of travel. This angular information is not lost when the cyclic tracking procedure of the MOCC/S solver is used, enabling comparisons with various angular approximations. Once again, the DRAGON cell code has been tested on a new class of benchmark problems with excellent results.

ACKNOWLEDGEMENTS

This research was supported by grants from the Natural Science and Engineering Research Council of Canada. We would like to thank Dr. Halsall for his help in providing all the necessary data.

REFERENCES

1. M. J. HALSALL, "Review of International Solutions to NEACRP Benchmark BWR Lattice Cell Problems," Report AEEW-R1052, Atomic Energy Establishment, Winfrith (1977).

2. G. MARLEAU, A. HÉBERT and R. ROY, "A User's Guide for DRAGON," Report IGE-174R3, École Polytechnique de Montréal (1997)..

3. R. ROY, "The Cyclic Characteristics Method," Int. Conf. Physics of Nuclear Science and Technology, Long Island, NY, Vol. 1, pp. 407-414 (October 5-8, 1998).

4. R. ROY, "Anisotropic Scattering for Integral Transport Codes. Part 2. Cyclic Tracking and its Application to XY Lattices," *Ann. nucl. Energy*, **18**, pp. 511-524 (1991).

5. T. JEVREMOVIC, T. POSTMA, J. VUJIC and K. TSUDA, "ANEMONA: Method of Characteristics based on the R-Function Two-Dimensional Solid Modeler," *Trans. Am. Nucl. Soc.* **79**, pp. 167-169 (1998); see also "A Comparative Study of the NEACRP Nine-Pin Supercell Benchmark by the Two-Dimensional General Geometry Transport Codes," *Trans. Am. Nucl. Soc.* **79**, pp. 169-171 (1998).

6. P.J. FINCK, C.G. STENBERG and R. ROY, "Development of a Reference Scheme for MOX Lattice Physics Calculations," *Trans. Am. Nucl. Soc.* **79**, pp. 299-301 (1998).

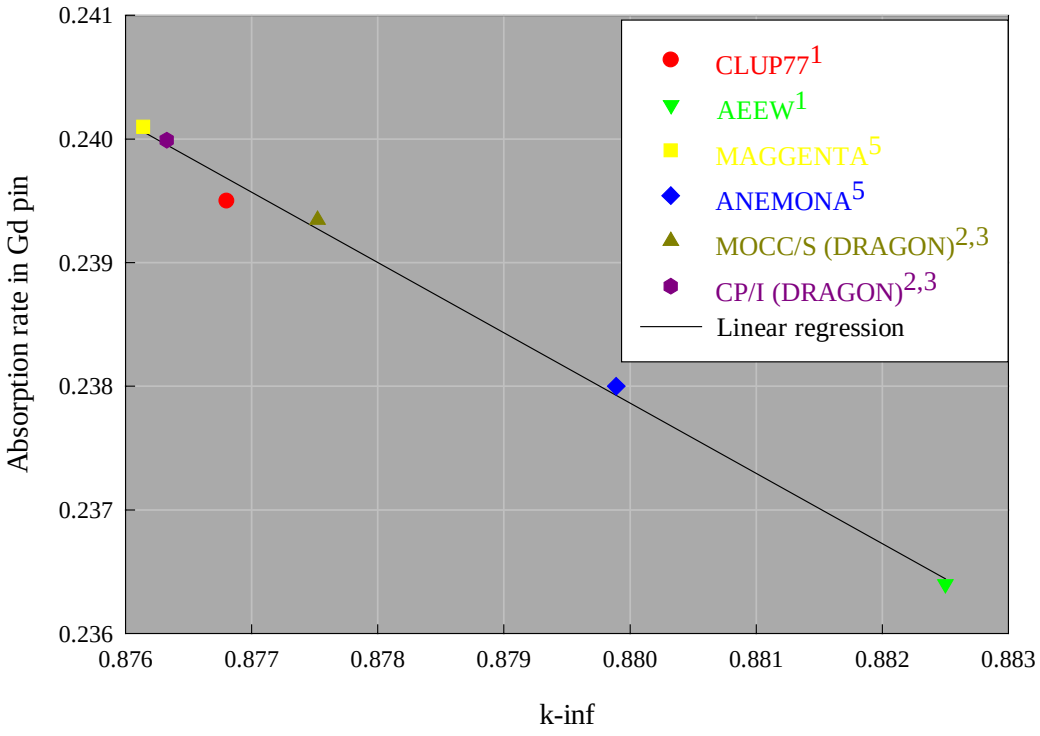

Figure 1. Total absorption rate in Gd pin versus k-infinite in Problem 1.

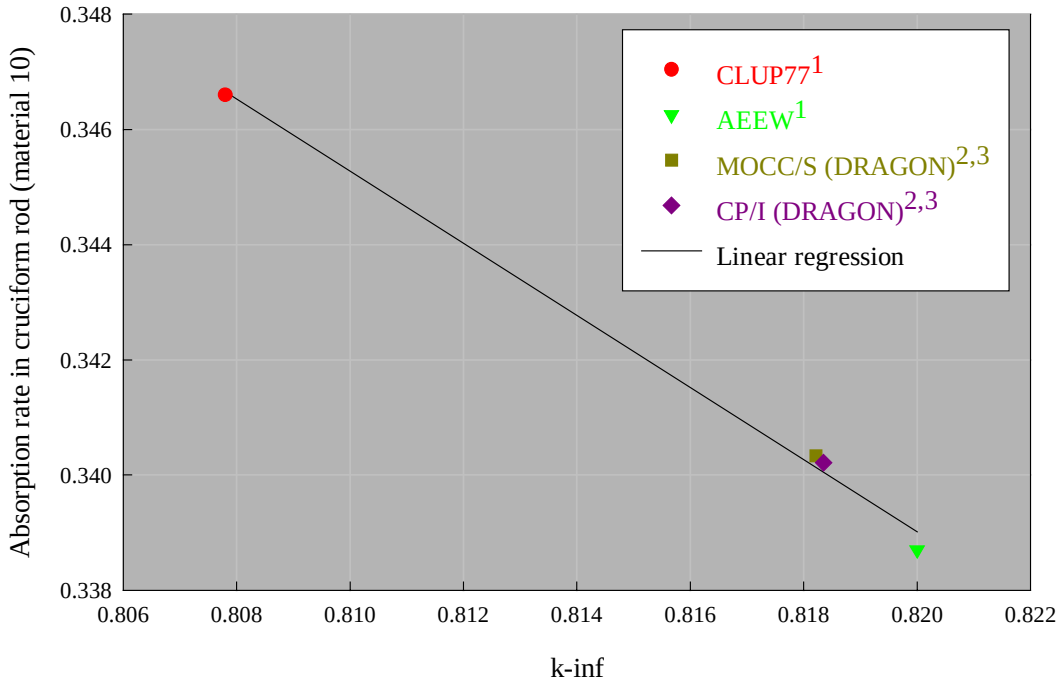

Figure 2. Absorption rate in cruciform rod versus k-infinite in Problem 2.